Available online at www.sciencedirect.com
SCIENCE DIRECT®
International Journal of Thermal Sciences 45 (2006) 29–40
International Journal of Thermal Sciences
www.elsevier.com/locate/ijts

Influence of a magnetic field on a single-plate thermoacoustic system

Shohel Mahmud *, Roydon Andrew Fraser

Department of Mechanical Engineering, University of Waterloo, 200 University Avenue West, Waterloo, ON N2L3G1, Canada

Received 4 September 2004; accepted 10 May 2005

Available online 16 June 2005

Abstract

In this paper, an analytical model for a single-plate thermoacoustic system in the presence of a magnetic field is proposed. The magnetic field acts perpendicular to the direction of the fluid oscillation. The governing momentum and energy equations are simplified to quasi-one-dimensional forms by approximations. Also these equations are used to derive the expressions for the fluctuating velocity (u_1), fluctuating temperature (T_1), Nusselt number (Nu_τ), and critical temperature gradient (∇T_{cr}) by a first order perturbation expansion. After the effects of Hartmann number (Ha_δ), drive ratio (DR), and temperature gradient (∇T_m) on the flow and thermal fields are discussed, they are graphically presented. Finally, for the present problem, a wave equation is modeled by using the continuity, momentum, and energy equations. In addition, some possible solutions to this equation are presented.

Keywords: Drive ratio; Hartmann number; Magnetohydrodynamics; Richardson's effect; Thermoacoustics; Wave equation

1. Introduction

A thermoacoustic interaction, the interaction between acoustic waves and temperature oscillations, is a rigid wall acoustic boundary layer phenomenon. Usually, a low Mach number compressible-viscous-oscillatory flow model [1–4] governs acoustic boundary layer transport interactions. Early mathematical treatments of a similar flow situation (an unsteady flow near a single-plate) date back to the works of Stokes [5]. Two classic problems: Stokes first problem, a suddenly accelerated plane wall; and Stokes second problem, flow near an oscillating flat plate, are the baseline for much of the subsequent analyses. Stokes first and second problems deal with an incompressible viscous flow only.

Interest in the interaction of compressible waves with motion that can be described as the flow of an incompressible fluid can be traced back to the 19th century. A curious phenomenon, presented by Leconte [6] in 1858 was the observation that the sound waves, produced by a musical instrument, modulate the flame of a gas burner. Kirchhoff [7] calculated the acoustic attenuation in a duct due to the oscillatory heat transfer between the solid isothermal duct wall and the gas sustaining the sound wave. Kirchhoff's [7] work is now considered to be an early analysis of what is now referred to as theoretical thermoacoustics. A well established theory on the interaction of sound waves with shear flows, far away from rigid walls, has been developed [8]; the theory's importance relates to the propagation of sound in the atmosphere or the ocean.

The early thermoacoustic theories, developed by Rott [9–14], are based on a linear expansion of the governing differential equations, and are usually applicable to a circular pore geometry with a large aspect ratio (= length/diameter). Rott's work, originally developed to investigate the Taconis oscillation [15], was the first linear theoretical investigation of heat driven oscillations. Rott's work [1] involves the calculation of the pressure, velocity, and temperature amplitudes; and the condition of the acoustic oscillation onset in a tube with both wide and narrow cross sections. He investigated a non-uniform temperature distribution [9], the relation between the temperature gradient in a tube and the onset of the oscillation [10], and heat the flux along the tube [11–13].

* Corresponding author.
E-mail addresses: smahmud@uwaterloo.ca (S. Mahmud), rafraser@uwaterloo.ca (R.A. Fraser).

1290-0729/$ – see front matter © 2005 Elsevier SAS. All rights reserved.
doi:10.1016/j.ijthermalsci.2005.05.002

Nomenclature

B	magnetic induction	$\mathrm{Wb\cdot m^{-1}}$
c	velocity of sound	$\mathrm{m\cdot sec^{-1}}$
C_f	skin friction coefficient (see Eq. (17))	
C_p	specific heat of the fluid at constant pressure	$\mathrm{J\cdot kg^{-1}\cdot K^{-1}}$
DR	drive ratio, $= P_A/p_m$	
E	electrical field intensity	$\mathrm{Volt\cdot m^{-1}}$
f	frequency of oscillation	Hz
Ha_δ	Hartmann number, $= B_y\delta_\nu\sqrt{\sigma/\mu}$	
i	complex number, $=\sqrt{-1}$	
J	current density	$\mathrm{amp\cdot m^{-2}}$
k_f	thermal conductivity of the fluid	$\mathrm{W\cdot m^{-1}\cdot K^{-1}}$
Nu_τ	complex Nusselt number (see Eq. (28))	
p	pressure	$\mathrm{N\cdot m^{-2}}$
P_A	amplitude of the fluctuating pressure	$\mathrm{N\cdot m^{-2}}$
Pr	Prandtl number of the fluid, $=\delta_\nu^2/\delta_k^2$	
Re_m	magnetic Reynolds number, $=\mu_0\sigma u_r\delta$	
T	temperature of the fluid	K
u	axial velocity component	$\mathrm{m\cdot sec^{-1}}$
V	velocity vector	$\mathrm{m\cdot sec^{-1}}$

Greek symbols

α_f	thermal diffusivity of the fluid	$\mathrm{m^2\cdot sec^{-1}}$
β	thermal expansion coefficient	$\mathrm{K^{-1}}$
δ_ν	viscous penetration depth, $=\sqrt{2\nu/\omega}$	
δ_k	thermal penetration depth, $=\sqrt{2\alpha_f/\omega}$	
δ^*	displacement thickness	m
μ	dynamic viscosity of the fluid	$\mathrm{N\cdot m^{-2}\cdot sec}$
μ_0	Permeability of the free space, $=4\pi\times10^{-7}$	$\mathrm{Wb\cdot amp^{-1}\cdot m^{-1}}$
ν	kinematic viscosity	$\mathrm{m^2\cdot sec^{-1}}$
σ	electrical conductivity of the fluid	$\mathrm{\Omega^{-1}\cdot m^{-1}}$
ω	circular frequency	$\mathrm{rad\cdot sec^{-1}}$
ρ	density of the fluid	$\mathrm{kg\cdot m^{-3}}$
τ	time period, $=2\pi/\omega$	
λ	wavelength	m

Subscripts and superscripts

1	first order variable
∞	free stream value
m	mean value
r	reference value
rms	root-mean-squared value

Symbols

$\Re[\,]$	real part of an expression
$\langle\Gamma\rangle$	time average of a complex expression Γ, $=\tau^{-1}\int_0^\tau \Gamma\,\mathrm{d}t$
Hg$\{\,\}$	hypergeometric function
$\mathbf{J}_{-\Psi}\{\,\}$	Bessel function of the first kind with order equals $-\Psi$
$\mathbf{Y}_{-\Psi}\{\,\}$	Bessel function of the second kind with order equals $-\Psi$

For a single-plate thermoacoustic system, Swift [2] developed an inviscid standing wave model which was modified for a traveling wave by Raspet et al. [16]. Both Swift [2] and Raspet et al. [16] derived expressions for the fluctuating temperature, and calculated the time averaged heat flux and work flux for their problems. Santillan and Boullosa [17, 18] included the effect of viscosity in the single-plate thermoacoustic model, developed by Swift [2] and Raspet et al. [16]. Swift et al. [19] discussed the possibility of using liquid metals as the working fluids in thermoacoustic engines, a consideration that opens the door in thermoacoustic for possibly using a magnetic force for the energy transfer. In their theoretical analysis, Swift et al. [19] selected liquid sodium due to its large thermal expansion coefficient, low Prandtl number, high density, and high electrical conductivity. Subsequently, Wheatley et al. [20] built a demonstration prime mover by using liquid sodium. The use of thermoacoustic prime movers with electrically conducting working fluids that transforms thermal gradient into electric power has also been proposed [21].

An important factor in the operation of thermoacoustic engines is time phasing which is similar to the traditional heat engines' piston-valve time-phase relationship. The key to phasing in thermoacoustic engines is the presence of two thermodynamic media: a working fluid and a solid plate. As the fluid oscillates along the plate at an acoustic frequency, the fluid undergoes changes in temperature. Some of the temperature change is the result of adiabatic compression and the expansion of the fluid caused by the sounds pressure waves, and some is a consequence of the local temperature of the plate itself. The heat flow between the fluid and plate does not produce instantaneous changes in the fluid temperature. Instead, the heat flow between the two media is subject to a time delay or time phasing which affects the temperature, pressure, and motion. Swift [2] stated that a poor thermal contact is necessary to achieve the proper phasing of the temperature oscillation of the working fluid. Magnetic force can also be used as a fluid oscillation and as a time phasing control mechanism in the vicinity of the plate. In general, the action of a transverse magnetic force on a conducting fluid is similar to that of a drag force [22]. Another important application of the combination of thermoacoustics and magnetic force is found in magnetic refrigerators [23] in the form of the magnetocaloric effect.

Although oscillatory boundary-layer flows have been studied in a number of MHD problems [24–27], the reported problems of a coupled MHD (magnetohydrodynamics) and thermoacoustics are rare. Recent studies by Ramos et al. [28, 29] are limited to a stability analysis of thermoacoustic oscillation in the presence of a magnetic filed.

In the present study, research is conducted to model and examine the effect of a transverse magnetic filed on the flow and thermal fields near a single-plate thermoacoustic system. A low Mach number compressible-viscous-oscillatory flow situation is considered. After the simplified governing differential equations are solved by the *complex exponential method* [30], the spatial and temporal distributions of the fluctuating velocity, temperature, and Nusselt number are presented.

2. Governing equations

Fig. 1(a) shows the schematic diagram of a simplified MHD thermoacoustic device used in this paper for analysis. To simplify the process, it is assumed that the acoustic wavelength (λ) is much longer than the dimensions of the plate (long-wave approximation), and that the acoustic pressure is much smaller than the mean pressure (small drive ratio, $|p_1| \ll p_m$). It is further assumed that the viscous and thermal penetration depths (δ_v, δ_k) are much smaller than the plate length. The general governing equations are:
continuity:

$$\frac{\partial \rho}{\partial t} + \nabla.(\rho \mathbf{V}) = 0 \tag{1}$$

momentum transfer:

$$\frac{\mathrm{D}\mathbf{V}}{\mathrm{D}t} = -\frac{1}{\rho}\nabla p + \nu \nabla^2 \mathbf{V} + \frac{1}{\rho}(\mathbf{J} \times \mathbf{B}) \tag{2}$$

heat transfer:

$$\rho C_p \left[\frac{\partial T}{\partial t} + \mathbf{V}.\nabla T\right] = k\nabla^2 T + \beta T \frac{\mathrm{D}p}{\mathrm{D}t} + \frac{|\mathbf{J}|^2}{\sigma} + \mu \Phi \tag{3}$$

and
electric charge transfer:

$$\nabla.\mathbf{J} = 0, \text{ where } \mathbf{J} = \sigma(\mathbf{E} + \mathbf{V} \times \mathbf{B}) \tag{4}$$

where $\mathbf{V}$, $\mathbf{J}$, $\mathbf{B}$, σ, Φ, and $\mathbf{E}$ are the velocity vector, volume current density, magnetic induction, electrical conductivity of the fluid, viscous dissipation function, and electric field intensity, respectively.

In a typical thermoacoustic problem, the product of the characteristic length (δ) and the permeability of the free space (μ_0) is very small ($\ll 1$), ensuring a low magnetic Reynolds number, $Re_m = \mu_0 \sigma u_r \delta$ (assuming a magnetic force is applied). In a low magnetic Reynolds number approximation, $\mathbf{B}$ influences $\mathbf{V}$ (via the Lorentz force), but $\mathbf{V}$ does not significantly perturb $\mathbf{B}$ [31]. Therefore, the induced magnetic field is negligible in comparison with the imposed field. When $Re_m \ll 1$, the magnetic field can be considered to be approximately equal to the imposed field. Since $\mathbf{B}$ is now almost constant, the electric field must be irrotational [31]; that is,

$$\nabla \times \mathbf{E} = -\frac{\partial \mathbf{B}}{\partial t} \approx 0 \tag{5}$$

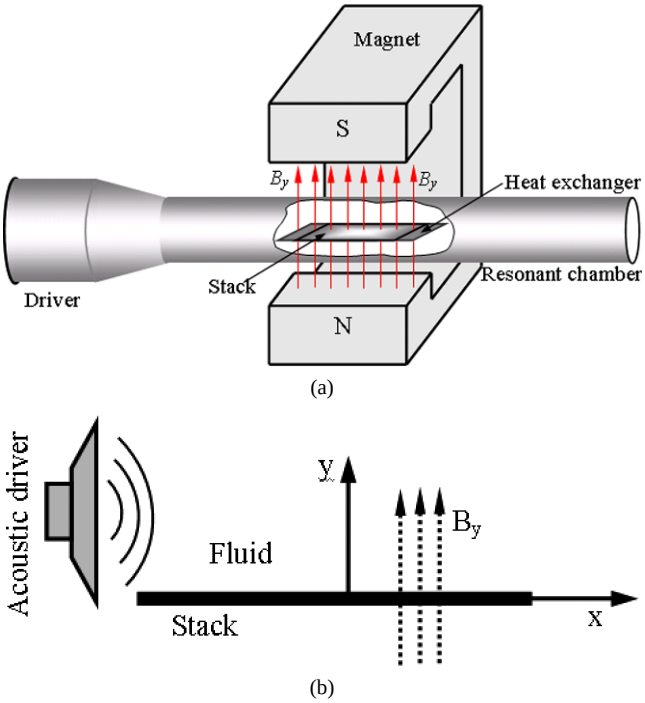

Fig. 1. (a) A schematic diagram of the problem under consideration and (b) analytical domain.

Ohm's law is now simplified to

$$\mathbf{J} = \sigma(-\nabla\varphi + \mathbf{V} \times \mathbf{B}) \tag{6}$$

where φ is the electrostatic potential. It should be noted that the behavior of the magnetic field at a very low Re_m is dissipative in nature, damping the mechanical motion by converting the kinetic energy into thermal energy via Joule dissipation [31].

3. Analysis of the flow field

It is assumed that there is a unidirectional shear flow ($\mathbf{V} \approx u(y)\hat{\mathbf{i}}$), adjacent to the stationary plate; therefore, a no-slip boundary condition is applicable at the plate surface. Far away from the plate, the fluid flow is uniform and the fluid velocity equals u_∞, depending on the time and other parameters (discussed later). The uniform imposed magnetic field ($\mathbf{B} \approx B_y\hat{\mathbf{j}}$) acts parallel to the y-axis as depicted in Fig. 1(b). By using these assumptions, the divergence of the electric field in Eq. (4) leads to the following expression:

$$\nabla.\mathbf{J} = -\sigma\nabla^2\varphi + \sigma\nabla.(B_y u\hat{\mathbf{k}}) = -\sigma\nabla^2\varphi + \sigma B_y \frac{\partial u}{\partial z} = 0 \tag{7}$$

which yields $\nabla^2\varphi = 0$. It is also assumed that there is no imposed electric field, and so $\varphi = 0$. Now the magnetic source term in Eq. (2) reduces to

$$\frac{1}{\rho}(\mathbf{J} \times \mathbf{B}) = -\frac{\sigma u B_y^2}{\rho}\hat{\mathbf{i}} \tag{8}$$

Any variable (for example, u, v, p, and T) can be expanded [1] as follows

$$\Phi = \Phi_m + \sum_{k=1}^{n} \Phi_k e^{ik\omega t} \tag{9}$$

The term with the subscript 'm' is the mean and with the subscript 'k' is the fluctuating part of that variable. ω represents the angular frequency which equals $2\pi f$, where f is the ordinary frequency. An expansion of Eq. (9) with $k = 1$, by using the linearized thermoacoustic theory [1,2], is sufficient for describing the simple thermoacoustic phenomena. Alternatively, any first order variable $\hat{\Phi}_1(y,t)$ can be expressed as

$$\hat{\Phi}_1 = \hat{\Phi}_1(y,t) = \Phi_1 e^{i\omega t} \tag{10}$$

If Eqs. (10) and (8) are substituted into Eq. (2) and only the first order terms are kept to yield

$$\frac{\partial^2 u_1}{\partial y^2} - \left\{ \frac{i\omega}{\nu} + \frac{\sigma B_y}{\mu} \right\} u_1 = \frac{1}{\mu} \frac{\partial p_1}{\partial x} \tag{11}$$

The solution to Eq. (11), after the boundary conditions, (a) $u_1(y=0) = 0$ and (b) $u_1(y \to \infty) =$ finite, are applied, yields

$$u_1 = \frac{i}{\rho_m \omega (1+\Psi)} \frac{\partial p_1}{\partial x} \left[1 - \exp\left(-\frac{1+i}{\delta_\nu} \sqrt{1+\Psi}\, y \right) \right] \tag{12}$$

In Eq. (12), Ψ equals $Ha_\delta^2/2i$ where Ha_δ is the Hartmann number and δ_ν is the viscous penetration depth, respectively. The viscous penetration depth $\delta_\nu (= \sqrt{2\nu/\omega})$ indicates how far the momentum can diffuse laterally during a characteristic time interval $(= 2/\omega)$. This time interval is of the order of the period of the oscillation $(\tau = 2\pi/\omega)$, divided by π. An expression of the oscillating free stream velocity $(u_{1,\infty})$ is obtained from Eq. (12) by the following:

$$u_{1,\infty} = \frac{i}{\rho_m \omega} \left(1 + \frac{i}{2} Ha_\delta^2 \right) \left(1 + \frac{1}{4} Ha_\delta^4 \right)^{-1} \frac{\partial p_1}{\partial x} \tag{13}$$

in terms of the fluctuating pressure gradient $(\partial p_1/\partial x$ or $\nabla p_1)$ and Ha_δ, respectively. Note that Eq. (13) is a simplified form of the parameters outside the square bracket at the right-hand side of Eq. (12). By using Eqs. (12) and (13), a non-dimensional fluctuating velocity is expressed as $u_1/u_{1,\infty}$. In such a case, y/δ_ν is a measure of the dimensionless transverse distance.

To model the pressure, a wave equation needs to be constructed by using the continuity and the momentum equations, and the thermodynamic relations. Modeling a wave equation depends on the specific type of thermoacoustic problem [1,2]. For the current problem, it is assumed that the stack is short enough that it does not perturb the standing wave appreciably (short stack approximation). Therefore,

$$p_1 = P_A \sin\left(\frac{x}{\tilde{\lambda}} \right) \quad \text{and} \quad \frac{\partial p_1}{\partial x} = \frac{P_A}{\tilde{\lambda}} \cos\left(\frac{x}{\tilde{\lambda}} \right)$$
$$\text{where } \tilde{\lambda} = \frac{\lambda}{2\pi} \tag{14}$$

In Eq. (14), λ is the wavelength, and P_A is the fluctuating pressure amplitude which depends on the drive ratio DR $(= P_A/p_m,\ p_m =$ mean pressure). The drive ratio (DR), which is a measure of the Mach number (Ma), is an important input parameter for thermoacoustic systems. If the Ma is defined as a ratio of the fluctuating velocity amplitude (u_a) to the velocity of sound (c_m) at the mean fluid temperature (T_m), the following expression,

$$Ma = \frac{u_a}{c_m} = \frac{\mathrm{DR}}{\gamma} \tag{15}$$

is a relation between the Ma and the DR where γ is the specific heat ratio $(= C_p/C_v)$ of the fluid. Two additional parameters; that is, the displacement thickness (δ^*) and the skin friction coefficient (C_f) are calculated according to White [32] and presented as follows:

$$\delta^* = \frac{1-i}{2} \frac{\delta_\nu}{\sqrt{1 - i\, Ha_\delta^2/2}} \tag{16}$$

and

$$C_f = \frac{1-i}{\delta_\nu} \frac{\rho_m \omega \nu}{\partial p_1/\partial x} \left(1 - i \frac{Ha_\delta}{2} \right)^{3/2}$$
$$= \frac{1-i}{\delta_\nu} \frac{\rho_m \tilde{\lambda} \omega \nu}{P_A} \left(1 - i \frac{Ha_\delta}{2} \right)^{3/2} \sec\left(\frac{x}{\tilde{\lambda}} \right) \tag{17}$$

Both δ^* and C_f are complex, but only the real parts of them have some physical meaning.

4. Analysis of the thermal field

In the cases where a linear expansion is adopted to expand the thermoacoustic variables (such as u, p, and T), the viscous dissipation and Joule heating terms in the energy equation (Eq. (3)) do not play any role, since they contain velocity (u and v) squared terms. By neglecting the effect of Joule heating and viscous dissipation on the heat transfer and by using a linear expansion, Eq. (3) is reduced to

$$\frac{\partial^2 T_1}{\partial y^2} - \left(\frac{i\omega}{\alpha_f} \right) T_1 = \frac{\nabla T_m}{\alpha_f} u_1 - \frac{i\omega\beta T_m}{\rho_m C_p \alpha_f} p_1 \tag{18}$$

where β, k_f, and C_p are the volumetric thermal expansion coefficient, thermal conductivity, and specific heat at constant pressure of the fluid, respectively. The general solution to Eq. (18) is

$$T_1 = C_1 \exp\left(\frac{1+i}{\delta_k} y \right) + C_2 \exp\left(-\frac{1+i}{\delta_k} y \right)$$
$$+ \Omega_1 \exp\left(-\frac{1+i}{\delta_\nu} \sqrt{1+\Psi}\, y \right) + \Omega_2 \tag{19}$$

where C_1 and C_2 are the two constants of the integration, and δ_k is the thermal penetration depth, respectively. The thermal penetration depth $\delta_k\ (= \sqrt{2\alpha_f/\omega})$ indicates how far the thermal energy can diffuse laterally during a characteristic time

interval ($=2/\omega$). In Eq. (19), Ω_1 and Ω_2 are two constants and are defined as

$$\Omega_1 = \frac{\nabla T_m \nabla p_1}{\omega^2 \rho_m (1+\Psi)} \frac{Pr}{Pr-(1+\Psi)} \tag{20}$$

and

$$\Omega_2 = \frac{\nabla T_m \nabla p_1}{\omega^2 \rho_m (1+\Psi)} - \frac{\beta T_m p_1}{\rho_m C_p} \tag{21}$$

After the following boundary conditions are applied: (c) $T_1(y=0)=0$ and (d) $T_1(y\to\infty)=$ finite, the expression of T_1, after a lengthy calculation, becomes

$$\begin{aligned} T_1 = {} & \left[\frac{\beta T_m p_1}{\rho_m C_p} - \frac{\nabla T_m \nabla p_1}{\omega^2 \rho_m (1+\Psi)}\right] \\ & + \left[\frac{\nabla T_m \nabla p_1}{\omega^2 \rho_m (1+\Psi)} \frac{Pr}{Pr-(1+\Psi)}\right] \\ & \times \exp\left(-\frac{1+i}{\delta_\nu}\sqrt{1+\Psi}\, y\right) \\ & - \left[\frac{\beta T_m p_1}{\rho_m C_p} + \frac{\nabla T_m \nabla p_1}{\omega^2 \rho_m} \frac{1}{Pr-(1+\Psi)}\right] \\ & \times \exp\left(-\frac{1+i}{\delta_k} y\right) \end{aligned} \tag{22}$$

where Pr is the Prandtl number of the fluid. Note that for the first temperature boundary condition (boundary condition (c)), it is assumed that the plate has a large enough heat capacity per unit area that its temperature does not significantly change at the acoustic frequency [2]. Since Eq. (22) is valid for $Ha_\delta \neq 0$ and $Pr \neq 1.0$, in the special case that $Pr=1$ and $Ha_\delta = 0$, the expression for T_1 becomes

$$\begin{aligned} T_1 = {} & \left[\frac{\beta T_m p_1}{\rho_m C_p} - \frac{\nabla T_m \nabla p_1}{\omega^2 \rho_m}\right]\left[1 - \exp\left(-\frac{1+i}{\delta_\nu} y\right)\right] \\ & + \frac{(1+i)\nabla T_m \nabla p_1}{2\omega^2 \rho_m}\left(\frac{y}{\delta_\nu}\right)\exp\left(-\frac{1+i}{\delta_\nu} y\right) \end{aligned} \tag{23}$$

In the limit of a large transverse distance, the negative exponential terms in Eq. (22) vanish, yielding an expression of the free-stream fluid temperature ($T_{1,\infty}$),

$$T_{1,\infty} = \frac{\beta T_m}{\rho_m C_p} p_1 - \frac{\nabla T_m}{\omega} \frac{\nabla p_1}{\omega \rho_m} \frac{1}{1+\Psi} = T_{\mathrm{ad}} - \frac{T_{\mathrm{sw}}}{1+\Psi} \tag{24}$$

The complicated expression of T_1 (Eq. (22)) requires a further analysis in order to achieve the physical interpretations of the different terms. Each of the three square bracketed terms represents a temperature amplitude factor [33]. The first square bracketed term is already identified in Eq. (24) as a free-stream fluid temperature ($T_{1,\infty}$). The first term of Eq. (24) represents a fluctuating temperature (T_{ad}) due to the adiabatic compression and expansion of the fluid [2]. The second term of Eq. (24) is derived from the mean-temperature gradient in the fluid; as the fluid oscillates along the x direction with an equivalent displacement amplitude u_0/ω (where $u_0 = \nabla p_1/\omega\rho_m$), the temperature, at a given point in space, oscillates by an amount $\nabla T_m u_0/\omega$, even if the temperature of a given volume of fluid remain constant. The $1+\Psi$ term denotes the influence of the magnetic field. In the absence of a plate (no y dependence in Eq. (22)) and with a zero mean temperature gradient ($\nabla T_m \approx 0$), T_1 in Eq. (22) reduces to T_{ad} which is, of course, desirable. The second and third square bracketed terms in Eq. (22) pose interpretation difficulties due to the complicated appearances of the different terms in them. However, the multiplied y-dependent terms (the complex negative exponential terms with δ_ν and δ_k) suggest that the second square bracketed term is a temperature amplitude factor with a hydromagnetic influence, and the third square bracketed term is a temperature amplitude factor with a thermal influence. For an inviscid fluid ($\mu \approx 0$) and in the absence of a magnetic force ($\Psi = 0$), Eq. (22) reduces to

$$T_1 = \left[\frac{\beta T_m}{\rho_m C_p} p_1 - \frac{\nabla T_m}{\omega} u_0\right]\left[1 - \exp\left(-\frac{1+i}{\delta_k} y\right)\right] \tag{25}$$

which is similar to the form that is obtained by Swift [2] for an inviscid single-plate thermoacoustic system. Note that Swift [2] used the standing wave features; that is, u_1^s and p_1^s, instead of u_0 and p_1 in Eq. (25). It is, however, a difficult task to obtain an expression for the non-dimensional fluctuating temperature from Eq. (22). $T_{1,\infty}$(or T_{ad}) can be used as a scale factor and the plate temperature (T_w) as a reference value to calculate the dimensionless temperature to be $(T_1 - T_w)/T_{1,\infty}$ or $(T_1 - T_w)/T_{\mathrm{ad}}$. Also y/δ_k is a measure of the dimensionless transverse distance. Note that the ratio of y/δ_k to y/δ_ν is equal to the square root of the Prandtl number ($\sqrt{Pr}$).

In Eq. (24), the fluid properties, temperature gradient, and flow properties can be written in such a way that the both terms on the right-hand side become equal, resulting in $T_{1,\infty} \approx 0$. In such a case, the resulting temperature gradient is proposed to be a critical temperature gradient (∇T_{cr}). Again, if a short stack approximation is assumed and only the real part of Eq. (24) is considered, then

$$\nabla T_{\mathrm{cr}} = \frac{1}{4}\left(1 + Ha_\delta^4\right)\frac{\beta T_m \omega^2 p_1}{C_p \nabla p_1} = \left[\frac{1+Ha_\delta^4}{4}\right]\frac{\beta T_m \omega p_1}{\rho_m C_p u_0} \tag{26}$$

Eq. (26) differs from Swift's [2] equation of critical temperature gradient originally derived for an inviscid ideal gas in a standing wave. Swift [2] obtained the following critical temperature gradient equation

$$\nabla T_{\mathrm{cr}} = \frac{T_m \beta \omega p_1^s}{\rho_m C_p u_1^s} \tag{27}$$

for an inviscid single-plate thermoacoustic system. As a viscous flow situation is considered in this paper, the definition of u_0 ($= \nabla p_1/\omega\rho_m$) in Eq. (26) differs from the definition of u_1^s in Eq. (27). Furthermore, the additional term, $(1+Ha_\delta^4)/4$, in Eq. (26) is a direct consequence of the magnetic field considered in this work but not by Swift [2]. In the limit of a vanishing viscosity and magnetic force, Eq. (26) reduces to Eq. (27). The origin of ∇T_{cr} derives from the fact that $T_{1,\infty} \approx 0$ in Eq. (24). Since there is a direct influence from the magnetic field (Ha_δ) on $T_{1,\infty}$, ∇T_{cr} is affected by

the change of Ha_δ as well. The motion of the fluid through a magnetic field induces an electric field that drives an electric current perpendicular to both the velocity and the magnetic fields. The interaction of this electric current and the applied magnetic field results in a Lorentz force [31] whose direction is always opposite to the velocity field in the absence of an applied electric field. The magnitude of the Lorentz force is higher in the free stream region [38]. The modification of the free stream velocity by the changing Lorenz force in turn affects the free stream temperature. In general, an increasing magnetic force increases the magnitude of the critical temperature gradient and vice versa.

5. Heat transfer and the Nusselt number

In the existing thermoacoustic literature, there is a very little about the Nusselt number. For example, Guoqiang and Ping [34] give an analytical expression for the complex Nusselt number in a circular pore. For a more complicated problem (a stack with two heat exchangers), Besnoin and Knio [35] numerically calculate the Nusselt number and show its variation with the heat exchangers' length. For the current problem, the following definition:

$$Nu_\tau = -\left(\frac{\delta_k}{T_w - T_{1,\infty}}\right)\left.\frac{\partial T_1}{\partial y}\right|_{y=0} \tag{28}$$

is used to calculate the complex Nusselt number. If T_1 is substituted into Eq. (28),

$$Nu_\tau = \frac{(1+i)}{T_{1,\infty}}\left[-\frac{\sqrt{1+\Psi}}{\sqrt{Pr}}\left\{\frac{\nabla T_m \nabla p_1}{\omega^2 \rho_m (1+\Psi)}\frac{Pr}{Pr-(1+\Psi)}\right\} + \left\{\frac{\beta T_m p_1}{\rho_m C_p} + \frac{\nabla T_m \nabla p_1}{\omega^2 \rho_m}\frac{1}{Pr-(1+\Psi)}\right\}\right] \tag{29}$$

which is valid for $Pr \neq 1$ and $Ha_\delta \neq 0$. In the special case of $Pr = 1$ and $Ha_\delta = 0$, the expression of Nu_τ becomes

$$Nu_\tau = \frac{(1+i)}{T_{1,\infty}}\left[\frac{\beta T_m p_1}{\rho_m C_p} - \frac{1}{2}\frac{\nabla T_m \nabla p_1}{\omega^2 \rho_m}\right] \tag{30}$$

6. Results and discussion

The terminology, interpretations, and simplifications of u_1, T_1, and Nu_τ have been presented in the previous sections. In this section, graphical results are given in order to understand the influence of different parameters (for example, $Ha_\delta, \nabla T_m$, and DR) on u_1, T_1, and Nu_τ. To avoid the confusion of the sign (+ or −), it is assumed that the plate is placed at the quarter wavelength ($0 \leqslant x \leqslant \lambda/4$) of the sound wave. Also, it is assumed that the ∇T_m is positive; that is, the cold heat exchanger is placed at the beginning of the plate (near the driver side) and the hot heat exchanger is positioned at the end of the plate. The thermophysical properties are assumed to be constant and are calculated at the mean temperature (T_m) except the mean density (ρ_m) which is calculated from the mean pressure (p_m). Most of the calculations are performed at the middle of the plate which equals $\lambda/16$ where λ is the wavelength. Although non-dimensional forms of the fluctuating velocity ($u_1/u_{1,\infty}$), temperature ($T_1/T_{1,\infty}$), and Nusselt number are adopted in this section, the properties of Helium at 298 K ($= T_m$) are used if it is necessary, but Helium has a low electrical conductivity.

6.1. Flow field

Figs. 2(a)–(c) depict the velocity profiles at various times during one oscillation. The time is measured in Figs. 2(a)–(c) from the point in the cycle when the particle undergoing oscillation is at its rightmost position over the plate. Nonzero viscosity results in a no-slip velocity between the boundary and the fluid which, in effect, produces a sheared velocity profile for the tangential velocity component. This sheared profile, as exhibited in Figs. 2(a)–(c), oscillates and its amplitude, at any given distance from the plate, changes with time. At a large distance from the plate, the fluid moves as if it is frictionless. One interesting feature of these velocity profiles is that they show a region near the stack in which u_1 is larger than $u_{1,\infty}$. Richardson and Tyler [36] reported similar behavior (Richardson's annular effect) of the velocity profile in a pipe. The effect can be understood realizing that the solution of Eq. (12) is, in effect, the superposition of a transverse wave and a uniform oscillation. The transverse wave has, at $y = 0$, a fluid velocity that is consistently equal and opposite to that of the uniform oscillation. For $y > 0$, however, the fluid velocity in the transverse wave can exceed its value at $y = 0$ and combine with the uniform velocity to produce, at some time during a cycle, a velocity that is larger for some values of y than the value of the uniform (free-stream) velocity. However, an increasing Ha_δ reduces the Richardson effect on the velocity profile (see Figs. 2(a)–(c)) and at a high Ha_δ (for example, $Ha_\delta = 10.0$), the Richardson effect is absent; that is, the maximum fluid velocity at a particular time equals $u_{1,\infty}$.

As previously mentioned, the fluid velocity is a superposition of $u_{1,\infty}$ (the uniform oscillation is independent of y) and $u_{1,y}$ (the transverse wave depends on y), where $u_{1,y}$ consists of $u_{1,\infty}$ times the negative exponential term. Due to the exponential decay, the effects produced by the plate on the velocity profile are not significant far away from the plate. Theoretically, u_1 approaches $u_{1,\infty}$ when y approaches ∞; however, the magnitude of u_1 is almost equal to $u_{1,\infty}$ within a distance that is slightly more than δ_ν. The following equation:

$$y = \Re\left[\ln(1 - u_1/u_{1,\infty})/\left\{(1+i)\sqrt{1 - i\,Ha_\delta^2}\right\}\right]\delta_\nu \tag{31}$$

gives a rough idea of how quickly u_1 approaches $u_{1,\infty}$ with an increasing δ_ν. For example, when $t = 0$ and $Ha_\delta = 0$, $u_1 \approx 0.9u_{1,\infty}$ at $y \approx 1.15\delta_\nu$ and $u_1 \approx 0.99u_{1,\infty}$ at $y \approx 2.3\delta_\nu$.

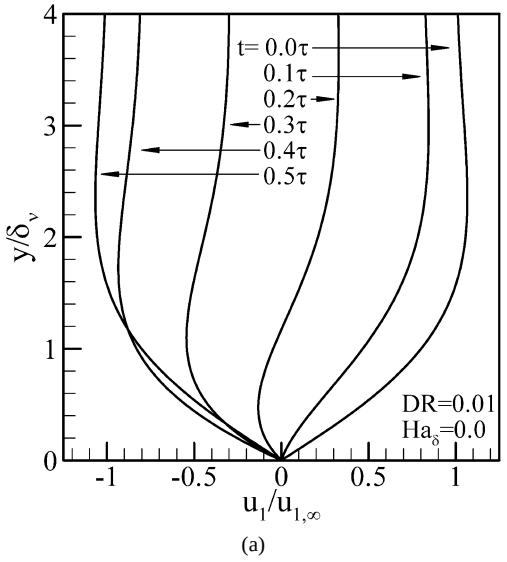

(a)

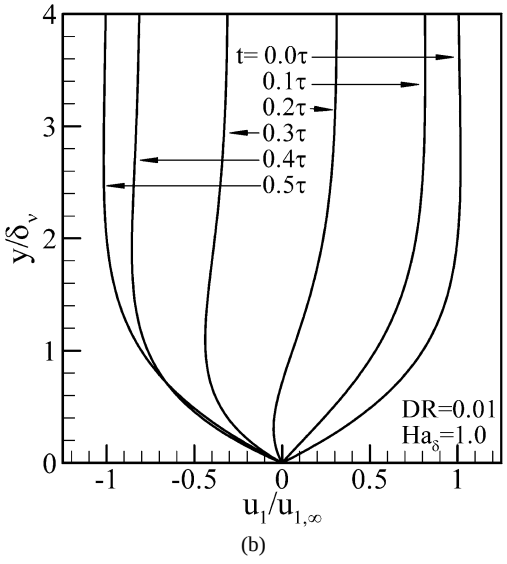

(b)

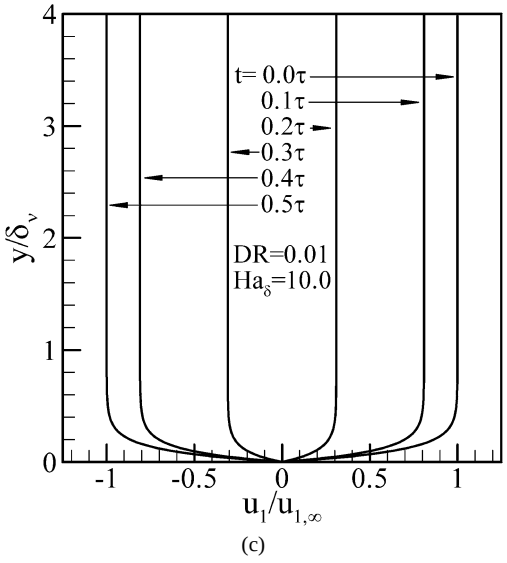

(c)

Fig. 2. The velocity profiles at different times during one cycle for $Ha = 0.0$, 1.0, and 10.0.

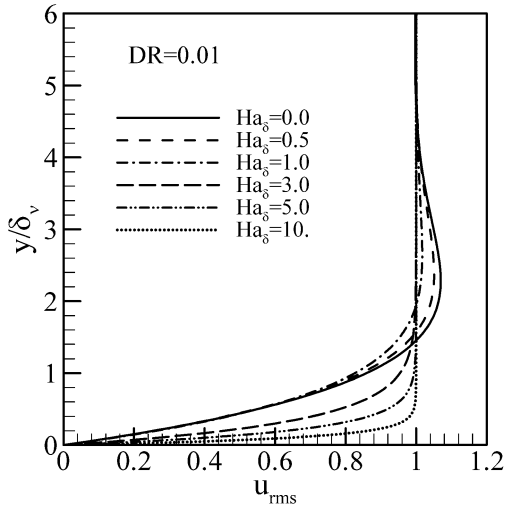

Fig. 3. The normalized average fluid velocity at different Hartmann numbers.

Since the reduction of the Richardson's effect is one of the consequences of an increasing Ha_δ, this tendency, along with some other effects of an increasing Ha_δ, can be understood if the non-dimensional form of the root-mean-squared velocity is computed as follows:

$$u_{\text{rms}} = \sqrt{\langle u_1^2 \rangle / \langle u_{1,\infty}^2 \rangle} \tag{32}$$

Fig. 3 displays u_{rms} as a function of y/δ_v at six selected Ha_δ. It is evident that the magnitude of the fluid velocity exceeds the free stream velocity only when $Ha_\delta \leqslant 1$. Hence, the Richardson effect does not exist, when $Ha_\delta > 1$. Another consequence of an increasing Ha_δ is the boundary layer thickness reduction. In the limit of an infinite Ha_δ, the boundary layer thickness becomes zero.

A close examination of Eq. (12) is required to understand the DR's effect on the velocity profile. In u_1 and $u_{1,\infty}$, the ratio of the fluctuating pressure gradient $(\partial p_1/\partial x)$ to the mean fluid density (ρ_m) is related to the DR by the following expression:

$$\frac{\partial p_1/\partial x}{\rho_m} = \text{DR}\left(\frac{RT_m}{\tilde{\lambda} M}\right)\cos\left(\frac{x}{\tilde{\lambda}}\right) \tag{33}$$

where M and R are the molecular weight of the fluid and the universal gas constant, respectively. Therefore, the higher drive ratio indicates a higher magnitude of the velocity, provided that the remaining parameters are constant. As the DR appears in $u_{1,\infty}$, the magnitude of $u_1/u_{1,\infty}$ is unaffected by the DR's variation. Fig. 4 displays the variation of the root-mean-squared skin friction coefficient $(C_{f,\text{rms}})$, as a function of Ha_δ, at different DRs. The $C_{f,\text{rms}} - Ha_\delta$ profiles are similar in shape for all the DRs. For $Ha_\delta \leqslant 1$, the variation in $C_{f,\text{rms}}$ is independent of the Ha_δ's variation, but for $Ha_\delta \geqslant 1$, the magnitude of $C_{f,\text{rms}}$ increases with the increases in Ha_δ. When $Ha_\delta \geqslant 1$, $C_{f,\text{rms}}$ decreases with the increases in the DR at a particular Ha_δ.

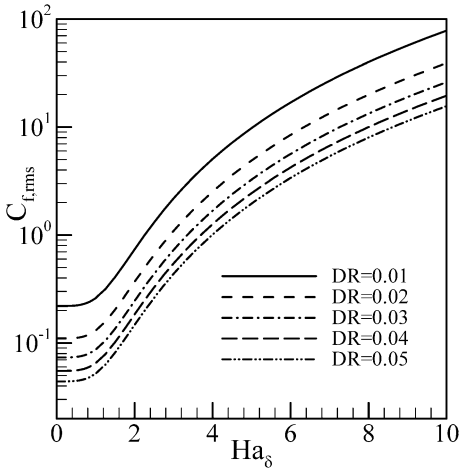

Fig. 4. The root-mean-squared skin friction coefficient at different drive ratios.

6.2. Thermal filed

For three different Ha_δ (= 0.0, 1.0, and 10), Figs. 5(a)–(c) display the non-dimensional temperature ($T_1/T_{1,\infty}$) profiles at various times during one oscillation. The DR and ∇T_m are kept constant. The fluctuating temperature is zero at the wall due the imposed boundary condition. Away from the wall, the temperature oscillates with time in a similar fashion to that of the velocity oscillation. Due to the vanishing negative exponential terms with an increasing y in Eq. (22), T_1 approaches $T_{1,\infty}$ at a distance that is equal to a few δ_k. Similar to Richardson's effect [35] on the velocity profile, Richardson's effect on the temperature profile indicates a maximum value ($> T_{1,\infty}$) in a region adjacent the plate. A close observation of Eq. (22) reveals that the temperature profile is a superposition of two transverse thermal waves and a uniform oscillation. Therefore, the discussion of Richardson's effect on the velocity profiles is applicable for the occurrence of the Richardson's effect-like case of the temperature profiles.

Ha_δ appears in T_1 in a very complicated way. An increasing Ha_δ has an insignificant influence on T_1, when ∇T_m is comparatively lower in magnitude. The $T_1/T_{1,\infty}$ profiles do not show any significant variation with an increasing Ha_δ, as depicted in Figs. 5(a)–(c) when $\nabla T_m = 1.0$. However, a considerable variation in T_1 is found when ∇T_m is high in magnitude as illustrated in Fig. 6. Here, the temperature profiles are shown only for $t = 0.0$. An increasing Ha_δ has a tendency to reduce each of the temperature components in Eq. (22); an increasing ∇T_m has a tendency to increase each of the temperature components in Eq. (22). With the definition of the ∇T_{cr} in Eq. (26), it is possible to express $T_1/T_{1,\infty}$ as

$$\frac{T_1}{T_{1,\infty}} = 1 + \frac{Pr}{(Pr-1)-\Psi}\frac{1}{\Gamma_0 - 1}\exp\left(-\frac{1+i}{\delta_v}\sqrt{1+\Psi}\,y\right) - \left[\Gamma_0 + \frac{1+\Psi}{(Pr-1)-\Psi}\right]\frac{1}{\Gamma_0 - 1}\exp\left(-\frac{1+i}{\delta_k}y\right) \tag{34}$$

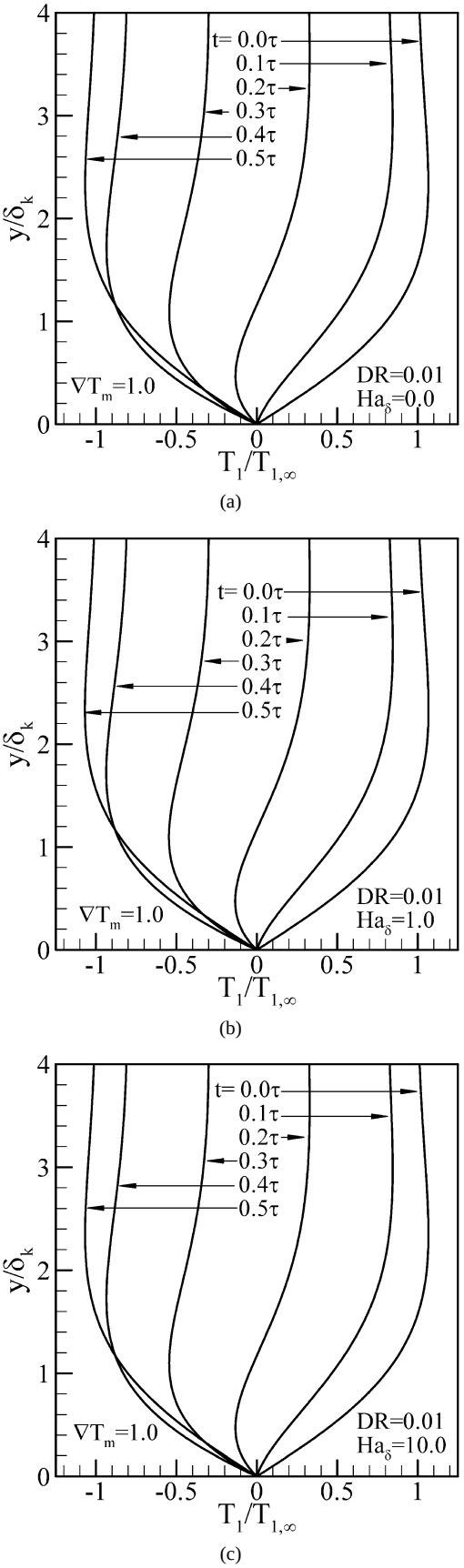

Fig. 5. The temperature profiles at different times during one cycle for $Ha = 0.0$, 1.0, and 10.0.

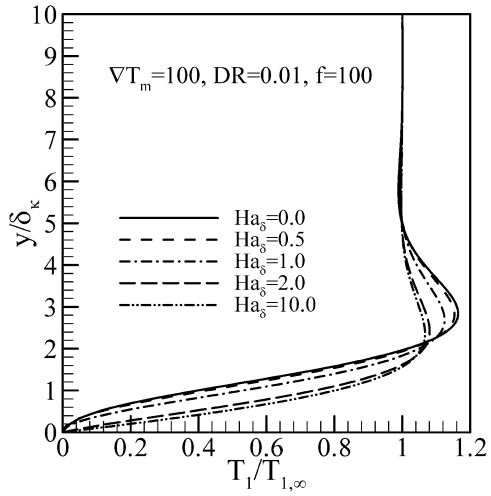

Fig. 6. The temperature profiles at different Hartmann numbers when $t = 0.0$ and $\nabla T_m = 100$.

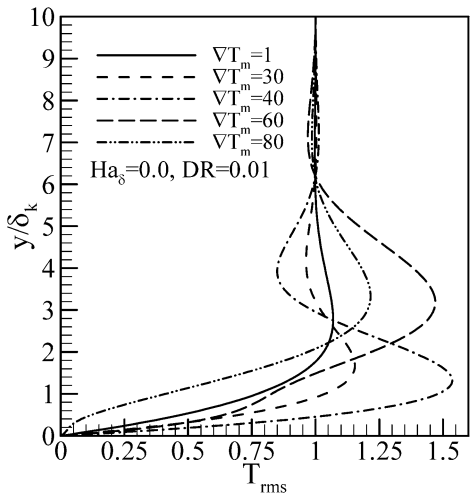

Fig. 7. The normalized average temperature at different Hartmann numbers.

where Γ_0 equals $\nabla T_{\rm cr}/\nabla T_m$. The inverse of Γ_0 is Γ[2]. The parameter, $\Gamma - 1$, is sometimes referred as a temperature gradient factor [2]. The $\nabla T_{\rm cr}$ is a combination of certain flow and fluid properties, and its variation is independent of the ∇T_m's variation. In the limit of small ∇T_m (that is, $\nabla T_m \ll \nabla T_{\rm cr}$), $\Gamma_0 \to \infty$, and Eq. (34) is reduced to the following form:

$$\lim_{\Gamma_0 \to \infty} \left(\frac{T_1}{T_{1,\infty}} \right) = 1 - \exp\left(-\frac{1+i}{\delta_k} y \right) \tag{35}$$

which is independent of Ha_δ. Therefore, at a low ∇T_m, the dimensionless temperature profiles are unaffected (or affected very little) by Ha_δ's variation (see Fig. 5). In the limit of a large ∇T_m (that is, $\nabla T_m \gg \nabla T_{\rm cr}$), $\Gamma_0 \to 0$, and Eq. (34) reduces to the following form:

$$\lim_{\Gamma_0 \to 0} \left(\frac{T_1}{T_{1,\infty}} \right) = 1 - \frac{Pr}{(Pr-1) - \Psi} \exp\left(-\frac{1+i}{\delta_\nu} \sqrt{1+\Psi}\, y \right) + \frac{1+\Psi}{(Pr-1) - \Psi} \exp\left(-\frac{1+i}{\delta_k} y \right) \tag{36}$$

which depends on Ha_δ. Therefore, at a high ∇T_m, the dimensionless temperature profiles are affected by the Ha_δ's variation (see Fig. 6).

In the expression T_1 in Eq. (22), each of the three terms on the right-hand side has a p_1 or ∇p_1 term. Since the DR appears indirectly in both p_1 and ∇p_1, $T_1/T_{1,\infty}$ is free from DR's influence. Next, the focus is on the influence of ∇T_m on the thermal field. In order to remove the time dependence of the temperature, the root-mean-squared temperature is calculated to become dimensionless as follows:

$$T_{\rm rms} = \sqrt{\langle T_1^2 \rangle / \langle T_{1,\infty}^2 \rangle} \tag{37}$$

Fig. 7 denotes the variation of $T_{\rm rms}$ as a function of y/δ_k at the different values of ∇T_m. $T_{\rm rms}$ is 0 at the wall as expected, regardless of ∇T_m's variation. $T_{\rm rms}$ approaches to its free stream value ($= 1$) as expected far away from the wall. As pointed our earlier, $\nabla T_{\rm cr}$ plays an important role for the temperature distribution. For the setting of the parameters in Fig. 7, $\nabla T_{\rm cr} \approx 50.8732$. When $\nabla T_m < \nabla T_{\rm cr}$, the near wall gradient of $T_{\rm rms}$ increases with increasing ∇T_m. This trend is reversed when $\nabla T_m > \nabla T_{\rm cr}$.

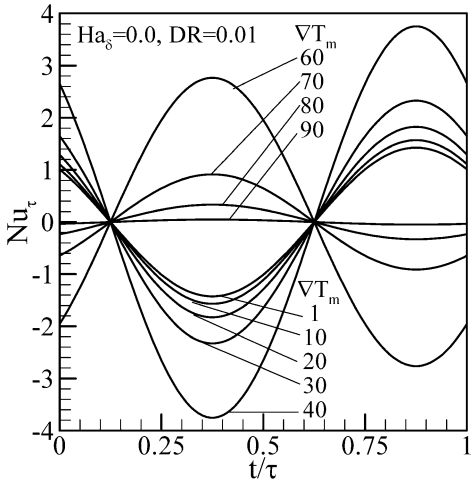

Fig. 8. The Nusselt number distribution as a function of time in one time period.

6.3. Heat transfer

Both Eqs. (29) and (30) are complex and time dependent. The appearance of p_1 and ∇p_1 in Eqs. (29) and (30) renders Nu_τ independent of DR's variation. For a constant Ha_δ and DR, Fig. 8 displays the time variation of Nu_τ at different ∇T_m's. One complete period ($t = 0 - \tau$) is selected to show Nu_τ's variation. Nu_τ exhibits a true periodic distribution with time with a zero time average ($\langle Nu_\tau \rangle = 0$) over a complete period. ∇T_m plays a critical role for Nu_τ's distribution. For the setting of the parameters in Fig. 8, $\nabla T_{\rm cr}$ ($\nabla T_{\rm cr} \approx 50.8732$) is computed from Eq. (26). Except at

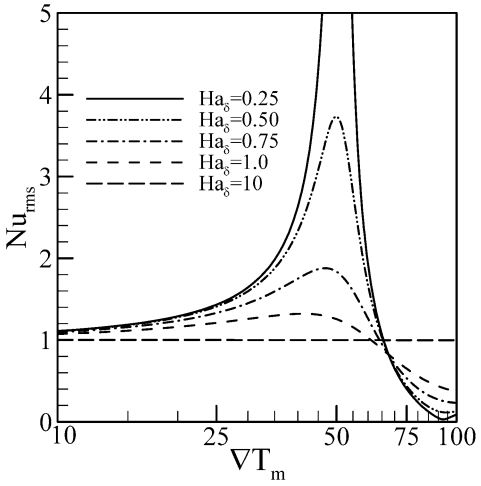

Fig. 9. The root-mean-squared Nusselt number as a function of the temperature gradient.

$t = 0.125\tau$ and 0.625τ, Nu_τ shows the opposite sign above and below the ∇T_{cr}; that is, at a particular time, Nu_τ is positive when $\nabla T_m > \nabla T_{cr}$, and negative when $\nabla T_m < \nabla T_{cr}$, and vice versa. Next, the root-mean-squared Nusselt number (Nu_{rms}) is calculated as the time average of Nu_τ, resulting in zero, in order to show its variation with Ha_δ and ∇T_m. Fig. 9 depicts the variation of Nu_{rms} as a function of ∇T_m at different Ha_δ. Theoretically, $\nabla T_m = \nabla T_{cr}$ is a singular point for Nu_τ's variation. The magnitude of Nu_{rms} is high at a value of ∇T_m close to ∇T_{cr}, as observed in Fig. 9. For the selected range of ∇T_m, ∇T_{cr} is more significant when $Ha_\delta < 1$. When $Ha_\delta > 1$, Nu_{rms} shows a minimal or no variation with ∇T_m's variation, and its value approximately equals 1.

7. Wave equation

Till this point, Eq. (14) has been used to express p_1 over the plate. Eq. (14) works well in the limit of a short-stack approximation. However, in more general cases, it is necessary to model and solve a wave equation in order to calculate the pressure fluctuation. The linearized first order continuity and inviscid momentum equations are

$$i\omega\rho_1 + \frac{\partial(\rho_m u_1)}{\partial x} = 0 \tag{38}$$

and

$$\left(i\omega\rho_m + \sigma B_y^2\right)u_1 = -\frac{\partial p_1}{\partial x} \tag{39}$$

By differentiating Eq. (39), with respect to x, and combining it with Eq. (38),

$$\rho_1 = -\frac{1}{\omega^2(1+\Psi)}\frac{\partial^2 p_1}{\partial x^2} \tag{40}$$

With the thermodynamic relation, $\rho_1 = -\rho_m\beta T_1 + (\gamma/c^2)p_1$, ρ_1 can be eliminated from Eq. (40) to yield

$$\frac{\partial^2 p_1}{\partial x^2} + \left(\frac{\omega\sqrt{\gamma}}{c}\sqrt{1+\Psi}\right)^2 p_1 - \rho_m\beta\omega^2(1+\Psi)T_1 = 0 \tag{41}$$

which is reduced to the following by using Eq. (24):

$$\frac{\partial^2 p_1}{\partial x^2} + (1+\Psi)\left(\frac{1}{T_m}\frac{\partial T_m}{\partial x}\right)\frac{\partial p_1}{\partial x} + (1+\Psi)\left[\left(\frac{\omega\sqrt{\gamma}}{c}\right)^2 - \frac{T_m\beta^2\omega^2}{C_p}\right]p_1 = 0 \tag{42}$$

By using the speed of sound and heat capacity thermodynamic relations, $c^2 = \gamma R T_m$ and $C_p = \gamma R/(\gamma - 1)$, the terms inside the square bracket of Eq. (42) are simplified to become $(\omega/c)^2$. Finally, the wave equation for the current problem becomes

$$\frac{\partial^2 p_1}{\partial x^2} + (1+\Psi)\frac{\partial \ln(T_m)}{\partial x}\frac{\partial p_1}{\partial x} + \left(\frac{\omega}{c}\sqrt{1+\Psi}\right)^2 p_1 = 0 \tag{43}$$

In Eq. (43), T_m depends on x and the sound speed (c) depends implicitly on x through its dependence on T_m. For a given $T_m(x)$, the numerical determination of p_1, from Eq. (43), presents no problem. However, great care should be taken to achieve an analytical solution to Eq. (43). Only very special distributions of $T_m(x)$ are appropriate for the analytic treatment of Eq. (43); for example, a piecewise constant temperature distribution [1] and a linear temperature distribution [16]. The first possible general solution to Eq. (43) can be obtained by assuming that the coefficients of $\partial p_1/\partial x$ and p_1 in Eq. (43) are constants. Then, the general solution to Eq. (43) is

$$p_1 = \tilde{A}_1\exp(\varphi_1 x) + \tilde{A}_2\exp(\varphi_2 x) \tag{44}$$

where the constants, $\tilde{A}_1$ and $\tilde{A}_2$, are real or complex expressions, and φ_1 and φ_2 are expressed as and

$$\varphi_1 = -\frac{1}{2}(1+\Psi)\frac{\partial \ln T_m}{\partial x} - \frac{1}{2}\sqrt{\left\{(1+\Psi)\frac{\partial \ln T_m}{\partial x}\right\}^2 - \left(\frac{2\omega}{c}\sqrt{1+\Psi}\right)^2} \tag{45a}$$

and

$$\varphi_2 = -\frac{1}{2}(1+\Psi)\frac{\partial \ln T_m}{\partial x} + \frac{1}{2}\sqrt{\left\{(1+\Psi)\frac{\partial \ln T_m}{\partial x}\right\}^2 - \left(\frac{2\omega}{c}\sqrt{1+\Psi}\right)^2} \tag{45b}$$

At the starting point of the plate ($x = x_s$), it is appropriate to apply the standing wave pressure $p_1^s(x_s)$. However, it is extremely difficult to apply correct boundary condition at the plate exit ($x = x_e$). None of the thermoacoustic literature covers such a boundary condition. In this situation, a more logical way is to apply the exit boundary condition that is similar to that of the fluctuating feature of a standing wave; that is, $p_1^s(x_e)$. Then, the expression of p_1 becomes

$$p_1 = \left[\frac{p_1^s(x_s)e^{\varphi_2 x_e} - p_1^s(x_e)e^{\varphi_2 x_s}}{e^{\varphi_1 x_s}e^{\varphi_2 x_e} - e^{\varphi_1 x_e}e^{\varphi_2 x_s}}\right]\exp(\varphi_1 x) - \left[\frac{p_1^s(x_s)e^{\varphi_1 x_e} - p_1^s(x_e)e^{\varphi_1 x_s}}{e^{\varphi_1 x_s}e^{\varphi_2 x_e} - e^{\varphi_1 x_e}e^{\varphi_2 x_s}}\right]\exp(\varphi_2 x) \tag{46}$$

where $p_1^s(x) = P_A \sin(x/\tilde{\lambda})$, $p_1^s(x_s) = P_A \sin(x_s/\tilde{\lambda})$, $p_1^s(x_e) = P_A \sin(x_e/\tilde{\lambda})$.

The applicability of Eq. (46) is restricted by the relations given in Eq. (45). To obtain a real result from Eq. (46), the following condition must be satisfied:

$$\frac{\partial \ln T_m}{\partial x} = \frac{\nabla T_m}{T_m} \geqslant \frac{2\omega}{c} \tag{47}$$

which, after further mathematical operations and simplifications, becomes

$$\nabla T_m \geqslant 4\pi \frac{T_m}{\lambda} = \frac{2T_m}{\tilde{\lambda}} \tag{48}$$

Next, a linear variation of temperature $T_m(x)$ is assumed as follows:

$$T_m(x) = T_c(1+mx), \quad \text{where } m = \frac{T_h - T_c}{T_c L} \tag{49}$$

In Eq. (49), T_h and T_c are the hot and the cold heat exchangers temperature, respectively, and L is the length of the plate. If it is further assumed that the variation of c is negligible with T_m's variation, the general solution to Eq. (43) is

$$p_1 = \tilde{A}_1 \exp\left(ik_0\sqrt{1+\Psi}\,x\right)(1+mx)^{-(1+\Psi)/2} \times \mathbf{Hg}\left\{\left[\frac{1+\Psi}{2}, \frac{1-\Psi}{2}\right], [\,], \frac{m}{2ik_0\sqrt{1+\Psi}(1+mx)}\right\} + \tilde{A}_2 \exp\left(ik_0\sqrt{1+\Psi}\,x\right)\mathbf{Hg}\left\{\left[\frac{1+\Psi}{2}\right], [1+\Psi], -\frac{2ik_0\sqrt{1+\Psi}(1+mx)}{m}\right\} \tag{50}$$

where k_0 equals ω/c. In Eq. (50), $\mathbf{Hg}\{\}$ is the generalized hypergeometric function [37]. If c varies with the temperature; that is, $c = \sqrt{\gamma R T_m(x)}$, the coefficient of p_1 is written as

$$\left(\frac{\omega}{c}\sqrt{1+\Psi}\right)^2 = \frac{k_1^2(1+\Psi)}{1+mx}, \quad \text{where } k_1 = \frac{\omega}{c_0} \tag{51}$$

In Eq. (51), c_0 is the velocity of sound at T_c. Now, the general solution to Eq. (43) becomes

$$p_1 = \left[\tilde{A}_1 \mathbf{J}_{-\Psi}\left\{2k_1\sqrt{\frac{(1+mx)(1+\Psi)}{m^2}}\right\} + \tilde{A}_2 \mathbf{Y}_{-\Psi}\left\{2k_1\sqrt{\frac{(1+mx)(1+\Psi)}{m^2}}\right\}\right] \times (1+mx)^{-\Psi/2} \tag{52}$$

where $\mathbf{J}_{-\Psi}\{\}$ is the Bessel function of the first kind [37] with the order $-\Psi$, and $\mathbf{Y}_{-\Psi}\{\}$ is the Bessel function of the second kind [37] with the order $-\Psi$.

8. Conclusions

The objective of the current research effort is to incorporate into the existing thermoacoustic theory a modification that uses a magnetic force as a non-contact controlling mechanism of the thermoacoustic effect. In the limit of a large transverse distance ($y \to \infty$), the fluctuating velocity and temperature approaches a $y-$independent free stream velocity and temperature, respectively. In reality, this large transverse distance is limited to a few δ_ν or δ_k. An increasing Hartmann number (that is, the increasing magnetic force) reduces the boundary layer thickness; in the limit of very large Hartmann number ($Ha_\delta \to \infty$), the boundary layer thickness becomes zero. The Richardson's effect (velocity u_1 is larger than $u_{1,\infty}$ in a region near the stack) is observed in the velocity profile only when $Ha_\delta \leqslant 1$. The variation of the non-dimensional axial velocity is independent of the drive ratio's variation. The fluctuating temperature profile shows a maximum ($> T_{1,\infty}$) in a region near the plate, similar to that of the velocity profile (the Richardson's effect-like scenario). The critical temperature gradient causes a zero free stream temperature for an appropriate combination of the fluid and flow properties. When ∇T_m is small, an increasing Hartmann number show a very little effect on the dimensionless temperature. However, a considerable variation of temperature is observed with Hartmann number's variation, when the mean axial temperature gradient is large. The Nusselt number indicates a periodic distribution with time, and its sign depends on the critical temperature gradient. For the selected range of the mean axial temperature gradients, the variation in the Nusselt number is insignificant with ∇T_m's variation; when $Ha_\delta < 1$. A wave equation is developed from the simplified continuity, momentum, and energy equations. Lastly, three possible solutions to the wave equation are presented.

References

[1] N. Rott, Thermoacoustics, Adv. Appl. Mech. 20 (1980) 135–175.
[2] G.W. Swift, Thermoacoustic engines, J. Acous. Soc. Amer. 84 (1988) 1145–1180.
[3] N. Cao, J.R. Olson, G.W. Swift, S. Chen, Energy flux density in a thermoacoustic couple, J. Acous. Soc. Amer. 99 (1996) 3456–3464.
[4] H. Ishikawa, D.J. Mee, Numerical investigation of flow and energy fields near a thermoacoustic couple, J. Acous. Soc. Amer. 111 (2002) 831–839.
[5] G.G. Stokes, On the effect of internal friction of fluids on the motion of pendulums, Math. Phys. Papers 3 (1901) 1–41.
[6] D.J. Tritton, Physical Fluid Dynamics, Oxford University Press, Oxford, 1988.
[7] G. Kirchhoff, Über den Einfluss der Wärmeleitung in einem Gas auf die Schallbewegung, Ann. Phys. (Leipzig) (2) 134 (1868) 177–193.
[8] M.J. Lighthill, Acoustic streaming, J. Sound Vibration 61 (1978) 391–418.
[9] N. Rott, Damped and thermally driven acoustic oscillations in wide and narrow tubes, Z. Angew. Math. Phys. 20 (1969) 230–243.
[10] N. Rott, Thermally driven acoustic oscillations. Part II. Stability limit for helium, Z. Angew. Math. Phys. 24 (1973) 54–72.

[11] N. Rott, The influence on heat conduction on acoustic streaming, Z. Angew. Math. Phys. 25 (1974) 417–421.
[12] N. Rott, The heating effect connected with non-linear oscillations in a resonance tube, Z. Angew. Math. Phys. 25 (1974) 619–634.
[13] N. Rott, Thermally driven acoustic oscillation. Part III. Second-order heat flux, Z. Angew. Math. Phys. 26 (1975) 43–49.
[14] N. Rott, Thermally driven acoustic oscillations, Part VI. Excitation and power, Z. Angew. Math. Phys. 34 (1983) 609–626.
[15] K.W. Taconis, J.J.M. Beenakker, A.O.C. Nier, L.T. Aldrich, Measurements concerning vapor-liquid equilibrium of solutions of ^{3}He–^{4}He, Physica 15 (1949) 733–739.
[16] R. Raspet, H.E. Bass, J. Kordomenos, Thermoacoustics of travelling waves: Theoretical analysis for an inviscid ideal gas, J. Acous. Soc. Amer. 94 (1993) 2232–2239.
[17] A.O. Santillan, R.R. Boullosa, Space dependence of acoustic power and heat flux in the thermoacoustic effect, Internat. Comm. Heat Mass Transfer 22 (1995) 539–548.
[18] A.O. Santillan, R.R. Boullosa, Acoustic power and heat flux in the thermoacoustic effect due to travelling plane wave, Internat. J. Heat Mass Transfer 40 (1997) 1835–1838.
[19] G.W. Swift, A. Migliori, T. Hofler, J. Wheatley, Theory and calculations for an intrinsically irreversible acoustic prime mover using liquid sodium as primary working fluid, J. Acous. Soc. Amer. 78 (1985) 767–781.
[20] J. Wheatley, G.W. Swift, A. Migliori, The natural heat engine, Los Alamos Science (1986) 2–29.
[21] G.W. Swift, A liquid–metal magnetohydrodynamic acoustic transducer, J. Acous. Soc. Amer. 83 (1988) 350–361.
[22] S. Mahmud, R.A. Fraser, Magnetohydrodynamic free convection and entropy generation in a square porous cavity, Internat. J. Heat Mass Transfer 47 (2004) 3245–3256.
[23] B.R. Gopal, R. Chahine, M. Foldeaki, T.K. Bose, Noncontact thermoacoustic method to measure the magnetocaloric effect, Rev. Sci. Instrum. 66 (1995) 232–238.
[24] W.I. Axford, Oscillating plate problem in magnetohydrodynamics, J. Fluid Mech. 8 (1960) 97–102.
[25] D.L. Turcotte, J.M. Lyons, Periodic boundary layer flow in magnetohydrodynamics, J. Fluid Mech. 13 (1962) 519–528.
[26] N. Datta, R.N. Jana, Hall effects on hydromagnetic flow over an impulsively started porous plate, Acta Mech. 28 (1977) 211–218.
[27] S. Cuevas, E. Ramos, Steady streaming in oscillatory viscous flow under a transverse magnetic field, Phys. Fluids 9 (1997) 1430–1434.
[28] E. Ramos, G. Huelsz, S. Cuevas, Effect of magnetic field on the linear stability of a thermoacoustic oscillation, in: Proc. 5th International PAMIR Conference on Fundamental and Applied MHD, Ramatuelle, France, September 16–20, 2002.
[29] E. Ramos, G. Huelsz, S. Cuevas, G. Ovando, MHD thermoacoustic oscillation in a waveguide filled with an electrolyte, in: Proc. World Congress on Ultrasonics (WCU-2003), Paris, France, September 7–10, 2003.
[30] L.W. Kinsler, A.R. Frey, A.B. Coppens, J.V. Sanders, Fundamental of Acoustics, Wiley, New York, 2000.
[31] P.A. Davidson, An Introduction to Magnetohydrodynamics, Cambridge University Press, Cambridge, 2001.
[32] F.M. White, Viscous Fluid Flow, McGraw-Hill, New York, 1991.
[33] S. Mahmud, R.A. Fraser, Flow and heat transfer inside porous stack: Steady state problem, Internat. Comm. Heat Mass Transfer 31 (2004) 951–962.
[34] L. Guoqiang, C. Ping, Friction factor and Nusselt number for thermoacoustic transport phenomena in a tube, J. Thermophys. Heat Transfer 14 (2000) 566–573.
[35] E. Besnoin, O.M. Knio, Numerical study of thermoacoustic heat exchangers in the thin plate limit, Numer. Heat Transfer (Part A) 40 (2001) 445–471.
[36] E.G. Richardson, E. Tyler, The transverse velocity gradient near the mouths of pipes in which an alternating or continuous flow of air is established, Proc. Roy. Soc. London A 42 (1929) 1–15.
[37] M. Abramowitz, I. Stegun, Handbook of Mathematical Functions, Dover, New York, 1965.
[38] U. Müller, L. Bühler, Magnetofluiddynamics in Channel and Containers, Springer, Berlin, 2001.